WALL STRUCTURE CHANGES IN LOW-LOSS MAGNETIC BUBBLE MATERIALS*

Bruce E. MacNeal† and Floyd B. Humphrey
California Institute of Technology, Pasadena, California 91125

Abstract

Transitions between underdamped and overdamped radial motion in magnetic bubble domains are investigated in a low-loss rare-earth garnet material. Three distinct types of domain wall structures, which are present during underdamped motion, have been identified. Bubble walls were subjected to a bias field pulse (H) and tested for underdamped motion sometime (τ) later. The first type of structure follows the form $H = H' \exp(\tau/\tau_o)$, with 170 nsec $< \tau_o <$ 270 nsec for the first transition, and is not statically stable. Transitions associated with the second type are characterized by a constant critical angle (Ψ_c) between the magnetization in the middle of the wall, and the plane of the wall. For the first transition, $\Psi_c = 230°$, and for the second, $\Psi_c = 370°$. These structures are statically stable. The third type of structure is not statically stable, and H is independent of τ. The first and second wall structure types are associated with multiple transitions while the third only exhibits a single transition.

Introduction

Structural changes in moving domain walls have been observed using a variety of experimental techniques [1,2]. It was found that domain walls move at a relatively high velocity for the first 15-40 nsec of wall motion, after which the walls move at a much lower velocity. This abrupt change in velocity was attributed to internal structural changes in the domain wall. Similar types of wall behavior were seen in bubble domains using a bubble collapse technique [3,4], and in strip domains, using a sampling technique [5]. Zimmer, et al also reported that rapid initial motion was only observed after the domain walls had remained stationary for several hundred nsec before the application of the drive field. Thus, structural changes appear to take place within the first few nsec of domain wall motion, but seem to produce effects on domain walls which persist for much longer times.

A different kind of structural transition has been reported in a recent study of domain wall oscillation in low-loss bubble materials [6]. Free bubbles were subjected to a step change in equilibrium radius, and, for small initial drive fields (<2.3 Oe), wall oscillation was observed. During wall oscillation, the domain wall velocity was constant, independent of the instantaneous drive on the wall. At a higher value of the initial drive field, H_T, the type of wall motion changed abruptly from underdamped to overdamped motion. As the initial drive was increased above H_T, underdamped motion slowly returned. At still higher drives ($\sim$4 Oe), a second transition to underdamped motion, similar to the first, was observed. A closer study of the first and second transitions showed small variations of H_T with static bias field, as well as slight differences between expanding and collapsing motion.

The present work examines the wall structures present in moving bubble domain walls in a low-loss garnet material. The structures are investigated by measuring the relationship between pulse amplitude and the time interval required to produce the transitions. Three different structures are identified by their distinct time dependences and statistical properties.

Experimental

A sampling optical microscope, described in detail elsewhere [7], was used to monitor the sizes of bubble domains. The microscope was modified to incorporate a Cohu - 4400 silicon-intensified target video camera for more convenient real-time observation. The camera and laser were synchronized to provide a 10 nsec single exposure image of the instantaneous size and shape of the bubble domains. Bias field pulses were provided by a pancake coil, driven by one or more HP 214A pulsers with a combined rise time of 12 nsec. Transitions between underdamped and overdamped motion were detected by monitoring the sizes of magnetic bubble domains at a fixed time during a bias field test pulse. Free bubbles were subjected to a 5 μsec long expanding bias field pulse with the pulse amplitude, H_o, set below the threshold for transitions. The delay of the sampling microscope was adjusted to take photographs of the bubble domains at the first time of maximum overshoot, typically 0.3 μsec after the beginning of the test pulse. Additional bias field pulses were applied at varying time intervals before the test pulse. These additional pulses were, under the proper conditions, able to produce overdamped motion during the test pulse. While executing overdamped motion, the size of a bubble at the time of maximum overshoot is smaller than it would be for underdamped motion, indicating directly whether it has executed underdamped or overdamped motion. Bubbles executing underdamped motion are typically 1 μm larger than those executing overdamped motion at this particular time, so that transitions are clearly visible on the TV monitor.

Two different bias pulse sequences were used to study transitions from underdamped to overdamped motion. In the first sequence, a step decrease in the bias field is applied at a time (τ) before the expanding test pulse. A sketch of this sequence is shown in Fig. 1. The experiment was performed by holding the values of τ and H_o constant while slowly increasing the step amplitude until an instability in bubble size was observed. This size instability indicates that bubbles are executing either underdamped or overdamped motion on a random basis. The pulse amplitude at which size instabilities were first observed is defined as the transition field for the step pulse sequence, $H_1(\tau, H_o)$. Size instabilities were observed over a range of 0.2 Oe in step amplitude, but H_1 was reproducible to within 0.04 Oe. In the second sequence a narrow collapsing pulse, or spike, of width W was applied a time (τ) before the beginning of the expanding test pulse. A sketch of this sequence is shown in Fig. 2. This experiment was performed by holding W, τ, and H_o constant, while slowly increasing the spike amplitude until size instabilities were observed. The spike amplitude at which instabilities were first observed is defined as the transition field for the spike pulse sequence, $H_2(\tau, W, H_o)$. Again, H_2 was reproducible to within 0.04 Oe. In either sequence, the test pulse amplitude is limited to values below H_T in order for the test pulse to be effective in detecting transitions. The time intervals (τ) are limited by the fact that bubble domains tend to distort at bias fields near the stripe-out field (19.0 Oe).

The bubble material used in these experiments is the same material investigated in an earlier study of domain wall oscillation [6]. Material parameters were determined through a combination of resonance measurements, giving α, $H_k - 4\pi M$, and γ, and measurements of

static domains, giving $4\pi M$, h, and ℓ. The results were $4\pi M = 93.5$ Oe, $\alpha = .009$, $h = 4.3$ μm, $\gamma = 18.3 \times 10^6 \text{Oe}^{-1}\text{s}^{-1}$, $\ell = 1.3$ μm and $H_k = 1080$ Oe. This sample exhibits a large amount of overshoot (~1 μm), and transitions between underdamped and overdamped motion are easily seen with the sampling optical microscope.

Results

The first transition field for the step pulse sequence (H_1) was measured as a function of the time interval (τ) with the test pulse amplitude (H_o) as a parameter. A typical result can be seen in the semi-log plot shown in Fig. 1. The pulse sequence is shown in the lower right corner of the figure. The static bias field was 23.0 Oe. Each data point represents a single determination of H_1, but in effect represents an average over several hundred repetitions of the same pulse sequence, since the sampling rate was 15 Hz and each measurement took at least 20 sec to complete. The transition field for $H_o = 0.0$ Oe is 2.47 Oe. Each set of data was fitted to a straight line, resulting in the relationship $H_1 = H' \exp(\tau/\tau_o)$. The results were: for $H_o = 1.3$ Oe, $H' = 1.30$ Oe, and $\tau_o = 270$ nsec. For $H_o = 1.5$, $H' = 1.13$ and $\tau_o = 230$. For $H_o = 1.7$, $H' = 0.95$, and $\tau_o = 190$. For $H_o = 1.9$, $H' = 0.83$, and $\tau_o = 170$. There is excellent agreement between the straight-line fits and the data except for $H_o = 1.9$ Oe. This deviation will be discussed later in connection with a second type of transition.

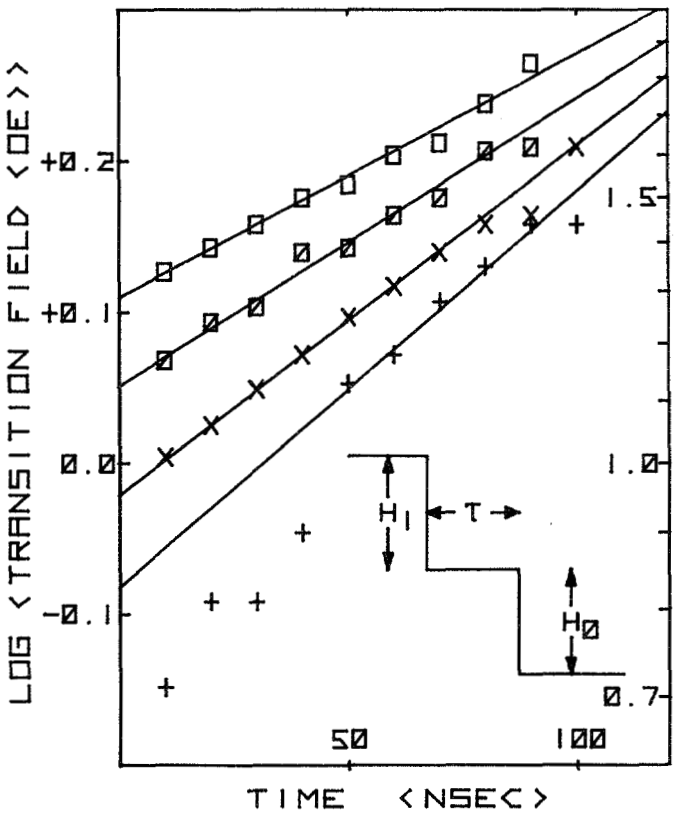

Fig. 1. Log_{10} (Transition Field (H_1) in Oe) vs Time Interval (τ, in nsec). For □, $H_o = 1.3$ Oe; for ⊠, $H_o = 1.5$; for X, $H_o = 1.7$; for +, $H_o = 1.9$. Step pulse sequence (shown). Static bias field = 23.0 Oe.

The transition field (H_1) was measured, using the same pulse sequence, for $H_o = 2.1$ Oe, and for $H_o = 2.3$ Oe, with markedly different results. In both cases the sums $H_1 + H_o$ were identical, and independent of τ, within experimental error. For $H_o = 2.1$ Oe, $H_1 + H_o = 2.60 \pm 0.05$ Oe, and for $H_o = 2.3$ Oe, $H_1 + H_o = 2.58 \pm 0.02$ Oe. For $\tau > 100$ nsec, shape distortions of the bubbles obscured the transitions. The statistical behavior for those transitions which are independent of τ near H_1 is different from that observed for the τ-dependent transitions. In the latter case, motion is always underdamped for pulse amplitudes slightly below H_1, and always overdamped slightly above H_1. In contrast, domain wall motion is underdamped on both sides of the weaker τ-independent transition, with at most a 50% probability of transition to overdamped motion in the center of the transition region.

The first and second transition fields for the spike pulse sequence (H_2) were measured as a function of the spike width (W) for fixed values of the time interval (τ). A typical result is shown in Fig. 2,

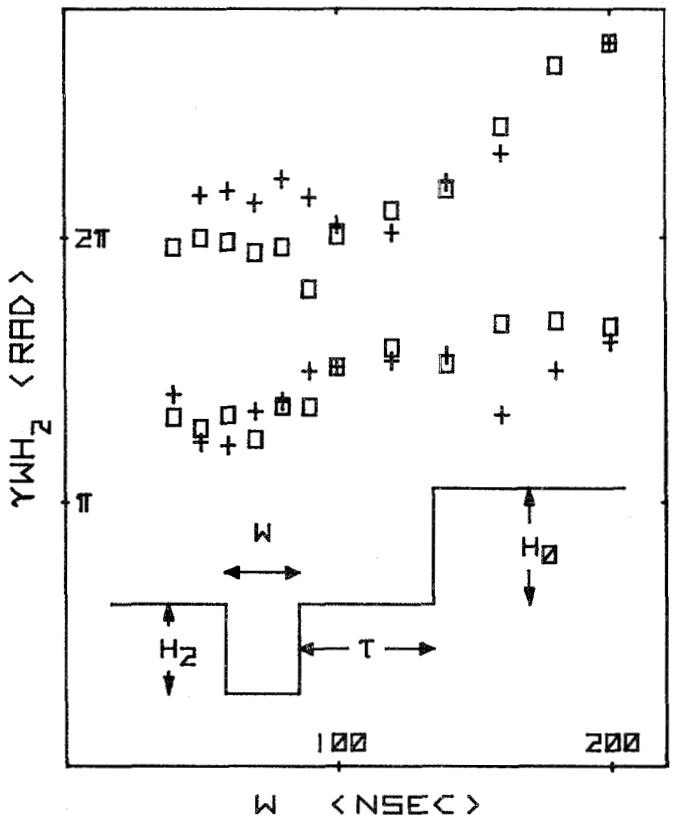

Fig. 2. γWH_2 (rad) vs W (nsec). For +, $\tau = 10$ μsec; for ⊠, $\tau = 2$ μsec. Spike pulse sequence (shown). Bias field = 24.0 Oe. $H_o = 1.7$ Oe.

where the product γWH_2 is plotted as a function of W for two values of τ. Again, the test pulse amplitude was 1.7 Oe, and the static bias field was 24.0 Oe. Both transitions correspond to a change from underdamped to overdamped motion. It can be seen that there is no significant difference in the product γWH_2 for the two different values of τ, except in the second transition for $W < 100$ nsec. For both transitions, γWH_2 is constant for $W < 100$ nsec. At higher values of W in the first transition, γWH_2 rises slightly and becomes constant again, while in the second transition, it also shows an increase, but does not assume a second constant value. The statistical distribution between underdamped and overdamped motion near both transitions using these larger values of τ is different from the distributions discussed earlier. Near a transition individual bubbles repeatedly execute the same type of motion, during successive repetitions of the same pulse sequence, and no bubble size instability is seen.

Every few seconds an individual bubble may convert from one type of wall motion to the other, but this conversion does not take place in the absence of the spike. With the spike and test pulse turned off each bubble remembers, for at least several minutes, which type of motion it was executing during the pulse sequence, and executes the same type of motion when the test pulse is turned on again. There is no significant difference in the d.c. collapse field between bubbles that execute different types of motion.

Discussion

Different wall structures, which cause transitions between underdamped and overdamped motion, may be identified by their distinct statistical properties, and by their different relationships between the transition field (H_1 or H_2) and the time interval (τ). The results reported here indicate that at least three distinct wall structures are present during underdamped domain wall motion. The first wall structure (type-I) is indicated by the results in Fig. 1. The contributions from H_1 and H_o are, at least partially, additive, since neither step change in bias field is large enough to cause transitions by itself. This also indicates that type-I structures are present during underdamped motion, since the step change in bias field (H_1) is not large enough to cause overdamped motion. The relationship between H_1 and τ is of the form $H_1 = H' \exp(\tau/\tau_o)$, with the relaxation times (τ_o) ranging between 170 nsec and 270 nsec. This relationship is observed even for τ = 10 nsec, indicating that type-I structures are created during the first few nsec of wall motion. The values of τ_o decrease with increasing H_o, indicating that the relaxation times for type-I structures depend on the "intensity" of the structures being detected by the test pulse. The times (τ_o) reported here are similar to those reported by Zimmer, et al[5]. They observed that the domain wall must remain stationary for at least 200 nsec before the bias field pulse in order for rapid initial motion to take place. These effects, Zimmer's and the one reported here, may result from the same type of wall structure, but are detected using different techniques.

A second type of wall structure (type-II) is indicated by the weak transitions observed during the step pulse sequence. The magnitude of the step change in bias field required to produce transitions (H_1) is independent of the time interval (τ), in contrast with the type-I transitions. For τ > 100 nsec, transitions due to type-II structures are not observed, and only type-I transitions are present. The statistical properties of the type-II transitions are different from those of the type-I transitions, being statistically weaker, and incomplete. Type-II structures are also created in the first few nsec of motion, since the relationship between H_1 and τ is preserved for τ = 10 nsec. For small values of τ and H_o, the values of H_1 for the two types of transitions are very close together, and may be confused. This fact accounts for the deviation shown in Fig. 1 in the data for H_o = 1.9 Oe, and for $\tau \leq 40$ nsec.

A third type of wall structure (type-III) is indicated by the transitions shown in Fig. 2. During the spike pulse sequence, the bubbles return to their original equilibrium radius before the test pulse is applied when long time intervals are used (τ=2 μsec and τ=10 μsec). Type-III structures are created during the spike and are statically stable, as indicated by the statistical behavior of the transition, and by the fact that H_1 is independent of τ. The two type-III transitions shown in Fig. 2 are characterized, approximately, by a constant value of $\gamma W H_2$. This suggests an interpretation of the transitions in terms of Slonczewski's formulation of wall motion [8]. In this formulation, the precession of the average angle between the magnetization at the center of the domain wall and the plane of the wall ($\bar{\psi}$) is given in terms of the effective drive field (H_e) and the wall velocity ($\dot{\bar{q}}$) by (Ref. 27, Eq. 2.15).

$$\dot{\bar{\psi}} = \gamma H_e - \frac{\alpha}{\Delta}\dot{\bar{q}}$$

where α is the resonance damping parameter, and $\Delta \equiv \sqrt{A/K}$. If the wall does not move appreciably during the spike, then $H_e \approx H_2$, and $\gamma H_e >> \alpha\dot{\bar{q}}/\Delta$. Thus, $\gamma W H_2$ represents the critical angle of rotation required to create type-III structures ($\bar{\psi}_c$). From Fig. 2, $\bar{\psi}_c$ = 230° for the first transition, and ψ_c = 370° for the second.

Conclusions

Two methods of producing transitions between underdamped and overdamped motion in a low-loss garnet material have been used to investigate domain wall structures present during underdamped motion. Three distinct types of wall structures have been identified by measuring their different time dependences and stability properties. One structure, created by fairly large bias field pulses, is stable, both statically, and in the presence of smaller bias field pulses. A second structure, created by moderate pulse amplitudes, decays exponentially with time, with relaxation times which are typically between 170 nsec and 270 nsec. A third structure, created by small pulses, does not decay measurably with time, but is also not statically stable. It is hoped that further investigations will give more information about the detailed nature of these structures.

Footnotes and References

* Supported in part by National Science Foundation Division of Materials Research Grant #DMR75-00420-A02.

† IBM Pre-doctoral Fellow

1. F. H. de Leeuw, J. Appl. Phys., 45, 1306 (1975).
2. F. H. de Leeuw and P. J. Rijnierse, AIP Conf. Proc. #18, 199 (1974).
3. S. Konishi, K. Mizuno, and K. Narita, J. Appl. Phys. 47, 3759 (1976).
4. G. P. Vella-Coleiro, AIP Conf. Proc. #24, 595 (1974).
5. G. J. Zimmer, L. Gál, and F. B. Humphrey, AIP Conf. Proc. #29, 85 (1975).
6. B. E. MacNeal and F. B. Humphrey, J. Appl. Phys., submitted for publication.
7. F. B. Humphrey, IEEE Trans., MAG-11, 1679 (1975).
8. J. C. Slonczewski, J. Appl. Phys., 44, 1759 (1973).